Journal of Hazardous Materials 171 (2009) 693–703

Contents lists available at ScienceDirect

Journal of Hazardous Materials

journal homepage: www.elsevier.com/locate/jhazmat

Characteristics of microporous/mesoporous carbons prepared from rice husk under base- and acid-treated conditions

Tzong-Horng Liou*, Shao-Jung Wu

Department of Chemical Engineering, Ming Chi University of Technology, 84 Gungjuan Rd., Taipei 24301, Taiwan

ARTICLE INFO

Article history:
Received 24 January 2009
Received in revised form 11 May 2009
Accepted 12 June 2009
Available online 21 June 2009

Keywords:
Rice husk
Activated carbon
Base-leaching
Acid-washing
Pore structure

ABSTRACT

The study reports the preparation of activated carbon with a high surface area from rice husk using chemical activation with H_3PO_4 and $ZnCl_2$. Activated carbon prepared from rice husk usually exhibits low specific surface areas due to its high ash content. However, experimental results show that base-leaching and acid-washing processes can effectively enhance the adsorption capacity of rice-husk carbon. The study also investigates the effects of preparation parameters on the surface characteristics of the carbon. These parameters include the kind of activating agent, before and after treatment procedures, impregnation ratio and activation temperature. The chemical and physical properties of samples were examined by EA, ICP-MS, XRD, FTIR, SEM and a N_2-adsorption meter. The surface areas obtained from $ZnCl_2$ and H_3PO_4 activation are as high as 2434 and 1741 m^2/g, respectively. These values are higher than that of activated carbon treated with neither base nor acid (1262 and 508 m^2/g for $ZnCl_2$ and H_3PO_4 activation). Thermogravimetric analysis shows that the activation process can be divided into three parts based on temperature zones. The results of this study will be useful in developing resource recovery systems for agricultural biomass.

1. Introduction

Activated carbon is a highly porous material with a large adsorption capacity. It is widely used in filtration and purification [1], catalyst supports and battery capacitors [2,3]. Activated carbon can also be used in gas storage for natural gas vehicles [4]. Environmental regulations have increased significantly in recent years, leading to an increased demand for activated carbon. Rice husk is a form of agricultural biomass constituent formed mainly from organic materials. Activating the rice husk in an inert atmosphere produces a highly porous carbon powder with a very high surface area. Since rice husk also has the advantages of being inexpensive and widely available, it is a very good candidate for preparing activated carbon.

Basically, there are two methods for preparing activated carbon: physical activation and chemical activation. Physical activation involves the carbonization of a precursor using a gaseous activating agent such as steam or CO_2 [5]. Chemical activation first mixes the precursor with a chemical activating agent such as phosphoric acid (H_3PO_4), zinc chloride ($ZnCl_2$) or alkali hydroxides (NaOH and KOH) and then heats it in an inert gas [6–9]. A comparison of chemical activation with physical activation shows that chemical activation provides a lower reaction temperature, and its global yield tends to be greater [10].

Rice husk is the by-product of the rice milling industry. Its constituent is complicated and contains an abundance of lignocellulosic biomass and ash. The ash contains approximately 99 wt% silica [11]. Developing countries around the world produce 500 million tons of rice annually [12]. Rice husk accounts for about 20% of the total weight of rice plants. Rice husk is bulky, and only a small portion of it is used as fuel. This creates a disposal problem as the amount is increasing year by year. Therefore, preparing a valuable material, such as activated carbon, from rice husk is a very interesting topic.

In general, the reported BET surface areas of activated carbon prepared from rice husk are 350–700 m^2/g by H_3PO_4 activation, and 500–1200 m^2/g by $ZnCl_2$ activation [13–17]. These surface area values are far lower than those of activated carbon prepared from other lignin–cellulose materials such as coconut shells, sugarcane bagasse, and hard wood. For example, activated carbon with a specific surface area of 1132 m^2/g has been prepared from sugarcane bagasse using H_3PO_4 activation [18], while $ZnCl_2$ activation produces a specific surface area of 2114 m^2/g for activated carbon prepared from coconut shells [19]. The lower surface area in rice-husk carbon is caused by its high ash content, whereas sugarcane bagasse and coconut shell have a relatively low ash content [20]. This ash can be removed by a base-leaching process [15]. After activation, the carbon precursor must be water-washed to remove any

* Corresponding author. Tel.: +886 2 29089899; fax: +886 2 29083072.
E-mail address: thliou@mail.mcut.edu.tw (T.-H. Liou).

0304-3894/$ – see front matter © 2009 Elsevier B.V. All rights reserved.
doi:10.1016/j.jhazmat.2009.06.056

chemical activating agents. However, the general water-washing process cannot effectively remove all chemical residues, and may also reduce the carbon's surface area. In this case, acid-washing is a viable alternative [21].

Many researchers have prepared activated carbon from coals, resins and lignin–cellulose materials. However, the preparation of activated carbon from rice husk using a base-leaching or acid-washing process has not been well studied to date. The primary objective of this study is to produce a highly porous activated carbon from rice husk by investigating the effects of various factors on the surface characteristic of the specimen. These factors include base-leaching and acid-washing procedures, the kind of activating agent, the activating agent impregnation ratio, and the activation temperature. The reactant and product obtained before and after the activation of samples are measured by SEM, XRD, FTIR, ICP-MS, EA and a N_2-adsorption analyzer. The thermal characteristics of the samples during activation are obtained using thermogravimetric analysis.

The method proposed in this study not only has the benefit of preparing activated carbon from carbonaceous matters with a high ash content, but may also be a potentially attractive method of producing advanced carbonaceous materials such as photocatalysts or bio-medical and nanoporous materials [22–25]. Simultaneously, it solves the problems of disposal and pollution created by burning rice-husk waste.

2. Experimental

2.1. Materials used and sample preparation

The raw material in this experiment was rice husk obtained from a rice mill. It was washed thoroughly with distilled water to remove soil and clay and then dried in air at 373 K in an oven for 24 h. Laboratory grade (Merck & Co.) H_3PO_4 and $ZnCl_2$ acted as activating agents, and NaOH and HCl acted as basic and acidic agents. The chemical composition of rice husk in the proximate analysis was 26.91 wt% of lignin, 34.56 wt% of cellulose, 22.18 wt% of hemi-cellulose, 5.81 wt% of moisture and 10.54 wt% of ash. Table 1 shows that the carbon, hydrogen, oxygen and nitrogen contents of the raw husk are 42.43%, 5.82%, 40.63% and 0.58% (w/w), respectively.

The process of preparing activated carbons from rice husk can be divided into three stages, which are illustrated as follows:

(1) *Base-leaching*. The dried rice husk was refluxed with a 1 M NaOH solution in a glass round-bottomed flask at 373 K within a thermostat. After the basic solution was drained, the rice husk was washed repeatedly with warm distilled water until the filtrate was free from the base, and then dried at 373 K for 24 h.
(2) *Activation*. The rice husk was impregnated with H_3PO_4 or $ZnCl_2$ and water at various ratios. The impregnation ratio is the mass of the activating agent compared to the mass of the dried rice husk. The impregnated husk was set in a sand bath at 423 K to remove excess water, and then oven-dried at 378 K for 24 h. A sample of the impregnated husk was then placed in a tubular reactor. Pure nitrogen gas (99.995%, San-Fu Chem. Co.) was used as a purge gas to ensure that the environment surrounding the sample was nonoxidizing. The reactor was inserted into a furnace and maintained at the desired temperature for 1 h.
(3) *Acid-washing*. After activating the samples, the husks were refluxed with a 3 M HCl solution at 373 K for 1 h [26]. After the acidic solution was drained, the samples were washed with hot distilled water several times to remove residual chemicals. The washed samples were dried at 378 K for 24 h, and then ground to form porous carbons.

Table 1
Elemental composition before and after the activation of samples.

	Composition, wt%					
	Water rinsed[a]	Base-leached[b]	H_3PO_4 activation[c]		$ZnCl_2$ activation[c]	
			UBUA	BA	UBUA	BA
C	42.43	44.27	66.21	76.87	80.02	82.71
H	5.82	4.76	4.52	4.45	2.50	2.72
O	40.63	49.91	20.87	15.38	13.81	14.10
N	0.58	0.23	0.16	0.14	0.14	0.37
Ash	10.54	0.83	8.24	3.16	3.53	0.10

[a] Sample was water-rinsed and un-heated.
[b] Sample was base-leached and un-heated.
[c] Samples were heated at 500 °C.

The description above shows that base-leaching and acid-washing are the first and last stages in preparing activated carbon, respectively. The experiment performed several tests to further determine the effects of base-leaching and acid-washing on sample surface characteristics. These tests consider several samples, as described below. The rice husk carbonized in N_2 only, without chemical activation, is called CRH. The rice husk (i) leached with a NaOH solution, (ii) activated with H_3PO_4 or $ZnCl_2$, and (iii) washed with a HCl solution, is called BA. The rice husk (i) leached with a NaOH solution, (ii) activated with H_3PO_4 or $ZnCl_2$, and (iii) washed with distilled water, is called BUA. The rice husk (i) washed with distilled water, (ii) activated with H_3PO_4 or $ZnCl_2$, and (iii) washed with distilled water, is called UBUA.

2.2. Analysis of organic elements and metallic impurities

The amount of fundamental organic element for various treatment procedures was determined using a Heraeus elemental analyzer. The dried sample was powdered to a mesh size (ASTM) of 325, and this powder was employed in the analysis. To measure the amount of metallic impurities in the samples, the reactant and product after activation were dissolved in a solution of HNO_3 and HF, and heated at 453 K for 6 h. The amount of metallic impurities in the solution was then determined with an inductively coupled plasma-mass spectrometer (ICP-MS) (Konton Plasmakon, model S-35).

2.3. Analysis of physical properties

The samples were characterized by specific surface area, pore volume and pore diameter. These values were measured at 77 K using the adsorption of nitrogen (Micrometric, model ASAP2010). The specific surface area of each specimen was calculated by the BET method in the relative pressure range of 0.01–0.1 [27]. This study assumes that the cross-sectional area for the nitrogen molecule is 0.162 nm^2. The single point total pore volume was determined from the amount of adsorbed nitrogen expressed as liquid state at a relative pressure of approximately 0.95. The micropore volume was estimated from the N_2-adsorption data using the Dubinin–Radush Kevich (DR) equation [28]. The average pore diameter was determined using the equation $4V/A$, where A is the BET surface area and V is the single point total pore volume [29]. This study defines micropores as having a width less than 2 nm, with mesopores and macropores being 2–50 nm and greater than 50 nm wide, respectively. The crystalline structures of the reactant and product were examined by an X-ray diffractometer (Siemens, model D-500) using Cu-Kα radiation at a scan speed of 2.5°/min. The morphology of the reactant and product was obtained with a scanning electron microscope (Topcon, model AST-150S). The composition of samples activated at various temperatures was measured using an infrared spectrometer (Shimadzu, model FTIR-8300).

Adsorption tests were conducted using iodine adsorption capacity. The known amount of activated carbon was placed into a flask containing 0.1N iodine solution, and then shaken to maintain equilibrium for 24 h. After adsorption, the adsorbent was removed by filtration. The iodine adsorption capacity was determined from the titration of the filtrate with a $Na_2S_2O_3$ solution.

This study also used a PerkinElmer TGA7 thermogravimetric analyzer to conduct experiments on the activation reaction of rice husk impregnated with the activating agent [30]. For each experimental run, a known weight of 6 ± 0.5 mg was placed on a platinum sample pan. The samples were heated to 1173 K at a rate of 10 °C/min in a nitrogen atmosphere. This study defines the remaining amount of sample decomposed in nitrogen as W/W_o, where W_o and W represent the initial and instantaneous mass of the sample, respectively. The TG and DTG curves were recorded simultaneously as the temperature increased.

3. Results and discussion

3.1. Analysis of organic elements and metallic impurities

Elemental analysis reveals changes in the rice-husk's organic element and ash content before and after activation. Table 1 indicates that the percentage of carbon element in the activated husks is higher than that in un-heated husks. However, hydrogen and oxygen elements follow the opposite trend. The decrease in oxygen and hydrogen contents may be attributed to the formation of water vapor, carbon dioxide, formic acid and acetic acid [31]. Comparing the water-rinsed and base-leached samples shows that the ash content decreased by more than 92 wt% after basic treatment of the rice husk. This is due to the fact that NaOH reacts with silica to form sodium silicate (Na_2SiO_3) [32]. The Na_2SiO_3 is soluble in water, and is removed by adequate water-washing. The overall reaction for Na_2SiO_3 formation is given by

$$2NaOH_{(s)} + SiO_{2(s)} \rightarrow Na_2SiO_{3(s)} + H_2O_{(l)} \quad (1)$$

When the rice husk is activated with H_3PO_4 or $ZnCl_2$, and neither base-leached nor acid-washed (UBUA), the ash content decreases. This indicates that silica reacts with the chemical activating agent. Comparing H_3PO_4 and $ZnCl_2$ activation shows that $ZnCl_2$ activation produces a higher carbonaceous content than H_3PO_4 activation, and the ash content is relatively lower as well.

Table 2 shows the amounts of metallic ingredients present in water-rinsed and activated samples. The water-rinsed sample has the highest concentration of Ca. When the rice husks are activated but not acid-washed (BUA), these metals can be removed by a simple water-washing procedure. It may be possible that the metals are carried by the vaporization of organic matter during pyrolysis.

Table 2
Amount of metallic ingredients before and after the activation of samples.

	Metallic ingredients as oxides, ppm				
	Water rinsed[a]	H_3PO_4 activation		$ZnCl_2$ activation	
		BUA[b]	BA[b]	BUA[b]	BA[b]
Mg	4,680	50	ND	255	56
Ca	15,460	402	142	95	68
Fe	750	604	85	57	48
Na	3,550	251	161	66	111
K	8,970	ND	19	ND	ND
Mn	1,800	ND	ND	ND	ND
P	5,430	97,600	30,700	470	ND
Zn	200	390	ND	31,400	ND
Total	40,840	99,297	31,107	32,343	283

[a] Sample was water-rinsed and un-heated.
[b] Samples were heated at 500 °C.

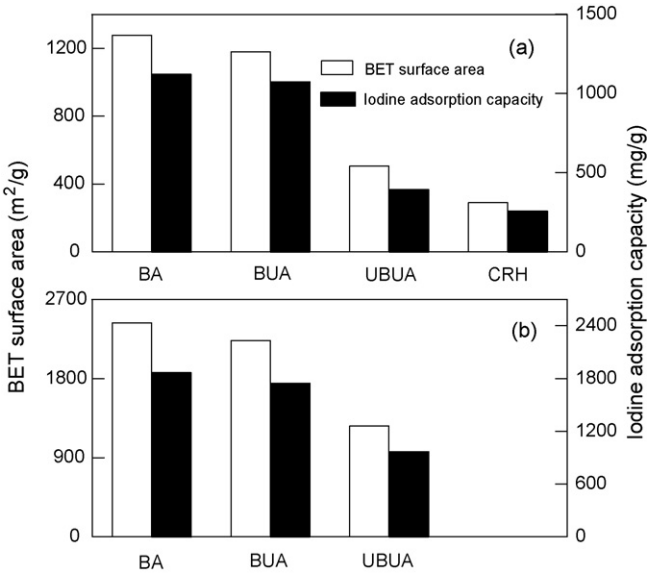

Fig. 1. Effect of base and acid treatment on surface area and iodine adsorption capacity of samples at impregnation ratio of 2: (a) H_3PO_4 activation at 400 °C and (b) $ZnCl_2$ activation at 500 °C.

However, the level of P and Zn in the BUA samples also increases seriously. Further, when the rice husks are treated with the acid-washing procedure (BA), impurities such as P and Zn are obviously reduced. This indicates that metallic impurities can be effectively removed by acid-washing. These results also show that Zn can be removed much more easily than P. The sample activated with $ZnCl_2$ has a higher purity than the H_3PO_4 activated sample. These observations show that the acid-washing procedure not only diminishes the native metallic impurity, but also removes the residual activating agent. This helps prevent the pore obstruction that leads to a reduction in adsorption capacity.

3.2. Analysis of reaction conditions

3.2.1. Effect of base or acid treatment process

Fig. 1 shows the effect of base or acid treatments on the BET surface area and iodine adsorption capacity of samples. The minimum BET surface area and iodine adsorption capacity occurs in the sample that is carbonized in nitrogen without being activated (CRH). When the rice husks are activated with H_3PO_4 or $ZnCl_2$, treated with neither base nor acid solution (UBUA), the two surface areas of H_3PO_4 and $ZnCl_2$ activation are increased. However, when the activated husks are treated with base-leaching but not acid-washing (BUA), the BET surface area and iodine adsorption capacity increase abruptly. Compared with the UBUA samples, the specific surface areas for BUA samples are almost doubled. When the activated husks are base-leached and acid-washed (BA), the BET surface area and iodine adsorption capacity reach their maximum. As mentioned earlier, rice husk contains a high ash content, and the component of ash is mainly silica. The EA analysis results in Table 1 show that silica can react with the activating agent, and its consumption may lead to a reduction in the activating agent/carbon ratio. This can contribute to a decrease in the surface area of the UBUA samples as well. Table 1 also shows that the ash content decreases significantly after the base-leaching process. This indicates that the disappearance of silica simultaneously creates more surface area and new pore structures. Yeganeh et al. [14] reported that the surface area of activated carbon depends on the ash content: the higher the ash content, the lower the N_2 surface area. Their observation is consistent with the present experimental results. Comparing the BA, BUA and UBUA samples shows that the base-

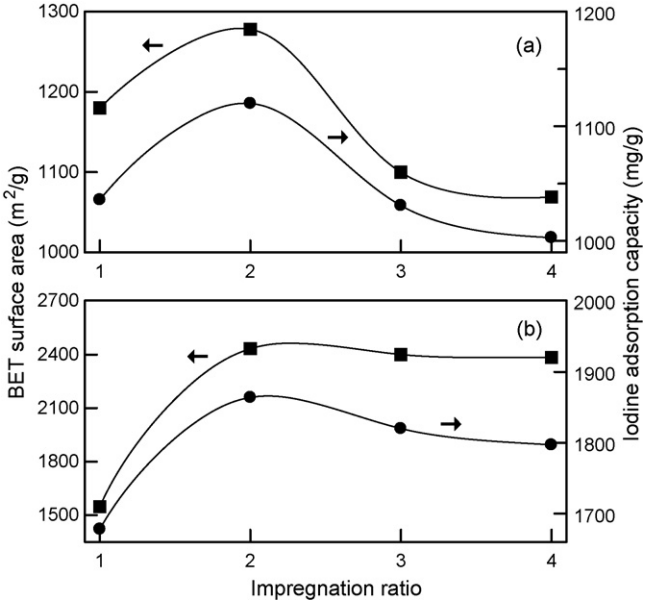

Fig. 2. Effect of impregnation ratio on the surface area and iodine adsorption capacity of samples: (a) H_3PO_4 activation at 400 °C and (b) $ZnCl_2$ activation at 500 °C.

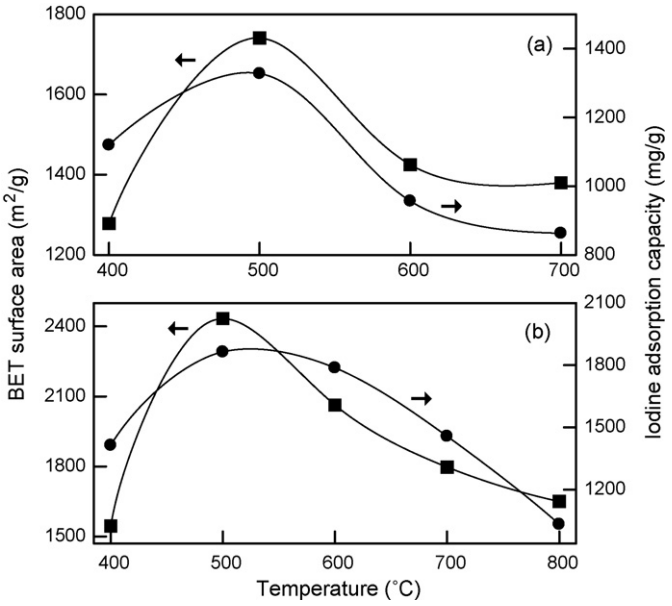

Fig. 3. Effect of activation temperature on the surface area and iodine adsorption capacity of samples at impregnation ratio of 2: (a) H_3PO_4 activation and (b) $ZnCl_2$ activation.

leaching procedure has a greater effect on enhancing the surface area and adsorption capacity than the acid-washing procedure.

3.2.2. *Effect of impregnation ratio of activating agent*

Fig. 2 shows the BET surface area and iodine adsorption capacity of rice husk activated with activating agent at various impregnation ratios. The surface area and adsorption capacity of both H_3PO_4 and $ZnCl_2$ activated husks reach their maximum value when the impregnation ratio is 2. However, the surface area is relatively small when the impregnation ratio is 1. This may be because activation occurs only at the exterior of the rice husk, and decreases the formation of pores. An increase in the activating agent promotes the contact area between rice husk and activating agent, and therefore, increases the surface area of carbon. When the impregnation ratio exceeds 2, the surface area of H_3PO_4 activated husk samples decreases, showing that these values are sensitive to the impregnation ratio. However, the surface area of $ZnCl_2$ activated husk samples is less affected when the impregnation ratio exceeds 2. The observation can be explained as follows. The porosity of the carbon structure can be created by removing the chemical activating agents in the carbonized samples. The N_2-adsorption capacity of activated carbon increases after washing with water [21]. However, in the case of H_3PO_4 activation, phosphate and polyphosphate species are incorporated into the carbon matrix through C–O–P bonds [33]. This indicates that part of the porosity of carbon samples is blocked by the phosphorus compounds, which are not easily removed with washing (as Table 2 implies). This situation leads to a decrease in surface area when too much H_3PO_4 is added to the husk. In the case of $ZnCl_2$ activation, the zinc salt left in the carbonized samples is highly soluble in water. This means that most of the $ZnCl_2$ is easily removed in the washing stage, indicating that the surface area does not change significantly at excess levels of $ZnCl_2$.

3.2.3. *Effect of activation temperature*

Fig. 3(a) shows that when rice husks were activated with H_3PO_4 from 400 to 700 °C, the BET surface area and iodine adsorption capacity of samples reach their maximum values at a temperature of 500 °C. When the activation temperature is lower than 500 °C, the reactants are only partial carbonized (as TGA thermograms indicate). As a result, the pores may not fully develop, decreasing the surface area. However, when the activation temperature is higher than 500 °C, violent gasification reactions may cause a part of the micropore structure to be destroyed by collapsing or combining together [34]. As a result, decreasing microporosity leads to an increase in mesopore volume. The surface area and adsorption capacity decrease when the reaction temperature exceeds 500 °C. These results are similar to the finding of other researchers [35] who reported that the surface area of carbon obtained from H_3PO_4 activation of rice husk reaches its maximum at a carbonization temperature of 450 °C. Fig. 3(b) shows that the reaction characteristics of $ZnCl_2$ activated samples have the same tendency as H_3PO_4 activated samples. The highest surface area also occurred at 500 °C. The $ZnCl_2$ activated samples have a higher BET surface area and iodine adsorption capacity than H_3PO_4 activated samples at the same reaction temperature. This is because Zn salts are easily removed in the washing stage after the activation reaction. However, P compounds are not easily removed due to the bonding of phosphorus and carbon in the activated sample. The pores for H_3PO_4 activated samples are not fully developed, and reduce the adsorption capacity. The optimum surface areas of carbons are 2434 m^2/g for $ZnCl_2$ activation and 1741 m^2/g for H_3PO_4 activation.

3.2.4. *Analysis of yield*

Fig. 4 plots the yield of carbon as a function of activation temperature and impregnation ratio for both H_3PO_4 or $ZnCl_2$ activated samples. The yield of activated carbon is determined using the relationship of Eq. (2). The standard deviations of the yield are on the order of around ±3%, and these values are used as the basis for the error bars shown in the figure.

$$\text{Carbon yield } (\%) = \frac{\text{mass of activated carbon}}{\text{mass of dried rice husk}} \times 100 \qquad (2)$$

Fig. 4(a) shows that the carbon yield for H_3PO_4 activation decreases as the impregnation ratio increases. This same trend appears in $ZnCl_2$ activated samples. This is because when the activating agent is increased, the chemical reaction between the rice husk and chemical agent becomes more violent. As a result, the vaporization of organic matter increases, reducing the yield. The yields for various chemical activating agents in Fig. 4(b) decrease as reaction temperature increases. By increasing the reaction tem-

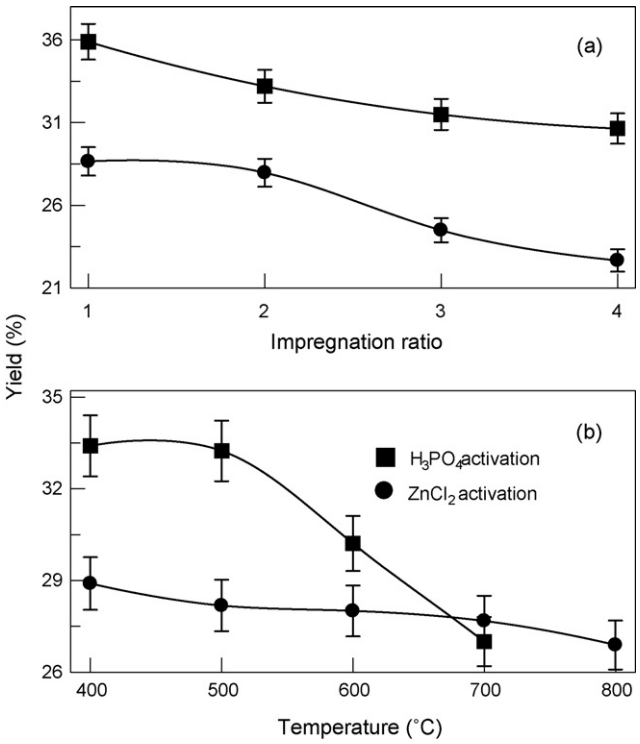

Fig. 4. Effect of activation temperature and impregnation ratio on carbon yield.

perature, the gasification becomes severe, and ultimately leads to a reduction in the yield. The yield values are lower than the activated carbon prepared from rice husk by the other workers, which are 37–41 wt% for H_3PO_4 activation [36], and 32 wt% for $ZnCl_2$ activation [10]. This is because the lignin tissue is removed after base-leaching the rice husk, and this causes a decrease in the carbon yield. For the same activation temperature and impregnation ratio, the carbon yield in the H_3PO_4 activation procedure is relatively higher than that obtained in the $ZnCl_2$ activation procedure. This can be explained by the fact that Zn salts are much more easily removed than P compounds in the activated carbons after the washing stage. Therefore, the chemical residues in the carbon lead to an increase in the carbon yield for H_3PO_4 activated samples.

3.3. Pore structure analysis

Fig. 5 shows the influence of the activation temperature and kind of activating agent on the nitrogen adsorption–desorption isotherms of the samples. According to the IUPAC classification [37], the carbon prepared from rice husk for both H_3PO_4 and $ZnCl_2$ activation exhibits a combination of types I and IV, showing the characteristics of microporous and mesoporous structures. Fig. 5(a) shows the results for samples activated with H_3PO_4 at various activation temperatures. When rice husk is carbonized without adding the chemical activating agent (CRH sample), the isotherm displays a sharp knee at the relative pressure (P/P_o) of about 0.01, and the plateau is nearly horizontal. This adsorption behavior indicates that the pore structure of carbonized rice husk is mainly microporous, with a narrow pore size distribution. When the H_3PO_4 activated sample is not base- or acid-treated (UBUA sample), it displays a sharp increase in knee and the slope of the plateau. The adsorption isotherm does not appear to contain a hysteresis loop, which indicates that the pore structure includes mostly micropores. The results of samples activated with H_3PO_4 at 400–600 °C display an abrupt increase in nitrogen uptake in the initial pressure range, indicating the formation of micropores. When the adsorption increases

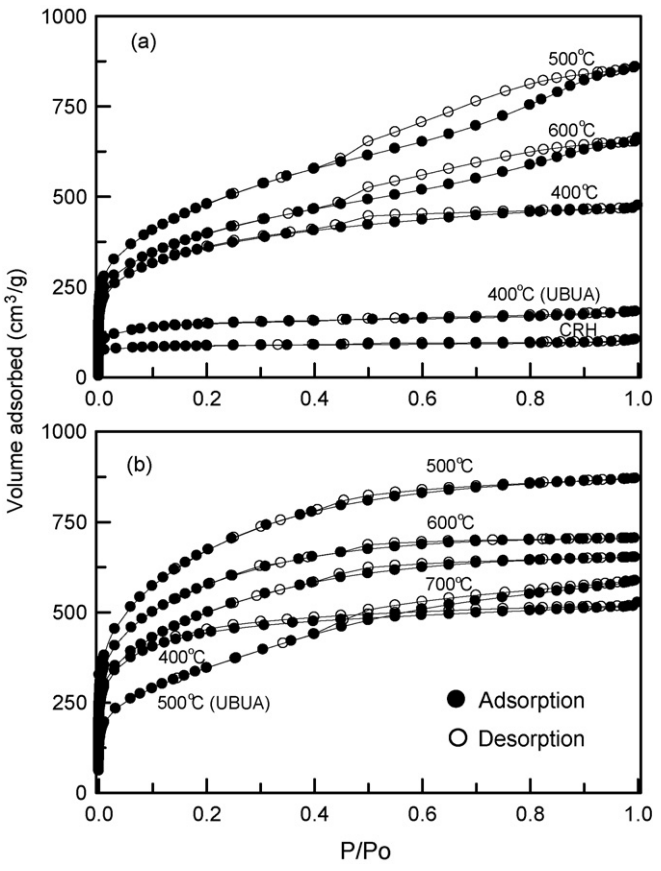

Fig. 5. Adsorption–desorption isotherm of samples at impregnation ratio of 2: (a) H_3PO_4 activation and (b) $ZnCl_2$ activation.

markedly above 0.4, the isotherms show apparent hysteresis loops. This may be caused by a capillary condensation in the mesoporous structures of the activated carbon. This implies that samples at various activation temperatures have both micropore and mesopore pore structures [11]. When the activation temperature is 500 °C, the adsorption capacity is at a maximum, indicating that the pore volume increases the most at this temperature.

Fig. 5(b) shows the results of the pore characteristics of samples activated with $ZnCl_2$ at various activation temperatures. When the activated rice husk is not base-leached or acid-washed (UBUA sample), a broad knee is observed with an increase in the slope of the plateau. The isotherm shows a slight hysteresis loop. This adsorption behavior indicates a mesoporous pore structure. The desorption hysteresis loop of samples activated with $ZnCl_2$ at 400–700 °C are not very obvious. The nitrogen adsorption capacities reach their highest values at an activation temperature of 500 °C. When the activation temperatures increase from 500 to 700 °C, the three isotherms display broad knees. The adsorbed volume gradually increases, suggesting that the pores are widened and the pore size distribution becomes broader [38]. These results also indicate that micropores and mesopores co-exist.

Table 3 illustrates the specific surface area and pore volume of rice-husk samples activated by various thermal treatment procedures. The pore structure of carbonized husk (CRH) is mainly microporous. This result agrees with the observation of Fig. 5(a). However, the pore volume is very small, at only 0.155 cm^3/g. When rice husks are activated with H_3PO_4 or $ZnCl_2$ but not acid or base-treated (UBUA), the pore volumes exhibit obvious increase. When activated rice husks are given acid and base treatments (BA), the pore volumes are higher than that of the UBUA process. This indicates that the ash and activating agent can be effectively removed

Table 3
Surface area and pore characteristics for carbonation and activation of samples.

	CRH[a]	H_3PO_4 activation					$ZnCl_2$ activation				
		UBUA[b]	400[c]	500[c]	600[c]	700[c]	UBUA[d]	400[c]	500[c]	600[c]	700[c]
S_{BET} (m^2/g)	292	508	1278	1741	1425	1380	1262	1545	2434	2062	1798
V_t (cm^3/g)	0.155	0.278	0.722	1.315	1.004	0.912	0.899	0.798	1.344	1.090	1.008
V_{mic} (cm^3/g)	0.116	0.193	0.366	0.286	0.286	0.293	0.268	0.463	0.590	0.473	0.415
V_{meso} (cm^3/g)	0.021	0.048	0.308	0.672	0.486	0.405	0.504	0.285	0.682	0.593	0.552
V_{mac} (cm^3/g)	0.018	0.037	0.048	0.357	0.232	0.214	0.127	0.050	0.072	0.024	0.041
D_p (nm)	2.13	2.19	2.26	3.02	2.82	2.75	2.85	2.06	2.21	2.11	2.24

S_{BET}, BET surface area; V_t, total pore volume; V_{mic}, micropore volume; V_{meso}, mesopore volume; V_{mac}, macropore volume; D_p, average pore diameter calculated as $4V/A$ by BET.
[a] Sample was heated at 500 °C.
[b] Sample was heated at 400 °C.
[c] Samples were treated with BA process at 400 °C–700 °C.
[d] Sample was heated at 500 °C.

after the pore structure is formed. This, in turn, increases the specific surface area and pore volume. For the H_3PO_4 activation procedure, the pore volume has a maximum value of 1.315 cm^3/g at an activation temperature of 500 °C. The sample exhibits significantly developed micropore and mesopore structures, with a higher proportion of mesopores than micropores. The $ZnCl_2$ activation procedure produces the same results as the H_3PO_4 activation procedure. The samples have a maximum pore volume of 1.344 cm^3/g at 500 °C. The pore structure shows the co-existence of both micropores and mesopores. The pore volume of the H_3PO_4 activation sample is close to that of $ZnCl_2$ activation sample at the same activation temperature. The average pore diameters of H_3PO_4 and $ZnCl_2$ activated samples range from 2.26 to 3.02 and 2.06 to 2.24 nm, respectively. The H_3PO_4 activated samples have a slightly higher pore diameter than $ZnCl_2$ activated samples.

3.4. Analysis of physical properties

Fig. 6 shows the X-ray diffraction analysis of rice husk and activated carbon samples prepared from H_3PO_4 or $ZnCl_2$ activation procedures at various activation temperatures. Fig. 6(a) shows the characteristic of fused silica in the raw material and CRH samples, with a diffraction peak around $2\theta = 22.5°$ [26]. The ash content disappears for all H_3PO_4 and $ZnCl_2$ activated samples at temperature ranges of 400–800 °C. Fig. 6(a) and (b) show no characteristic peaks after activation, indicating that the activated carbon samples obtained using both H_3PO_4 and $ZnCl_2$ activation procedures exhibit the turbostratic structure of disordered carbon materials [39]. However, there are two broad peaks around $2\theta = 25°$ and 45°. Similar patterns were obtained for carbon precursors heated at all temperatures. The peak near $2\theta = 45°$ shows a narrowing with increasing temperature, which indicates an increase in the lattice size. Experimental results also show that the peak intensity of samples using the $ZnCl_2$ activation procedure (Fig. 6(b)) is higher than that using the H_3PO_4 activation procedure (Fig. 6(a)). This indicates that the carbon obtained by $ZnCl_2$ activation has a relatively large size of crystallite.

To qualitatively characterize the surface groups on raw husk and activated carbon, the study analyzed FTIR spectra, as Fig. 7 indicates. This spectrum of raw material has a lot of similarities with

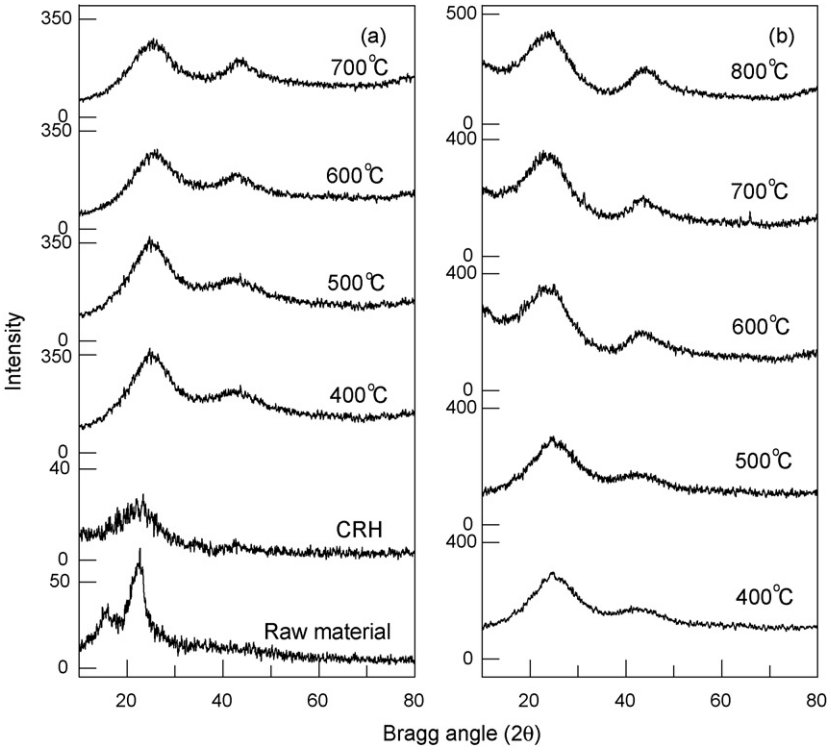

Fig. 6. X-ray diffractogram of samples: (a) H_3PO_4 activation and (b) $ZnCl_2$ activation.

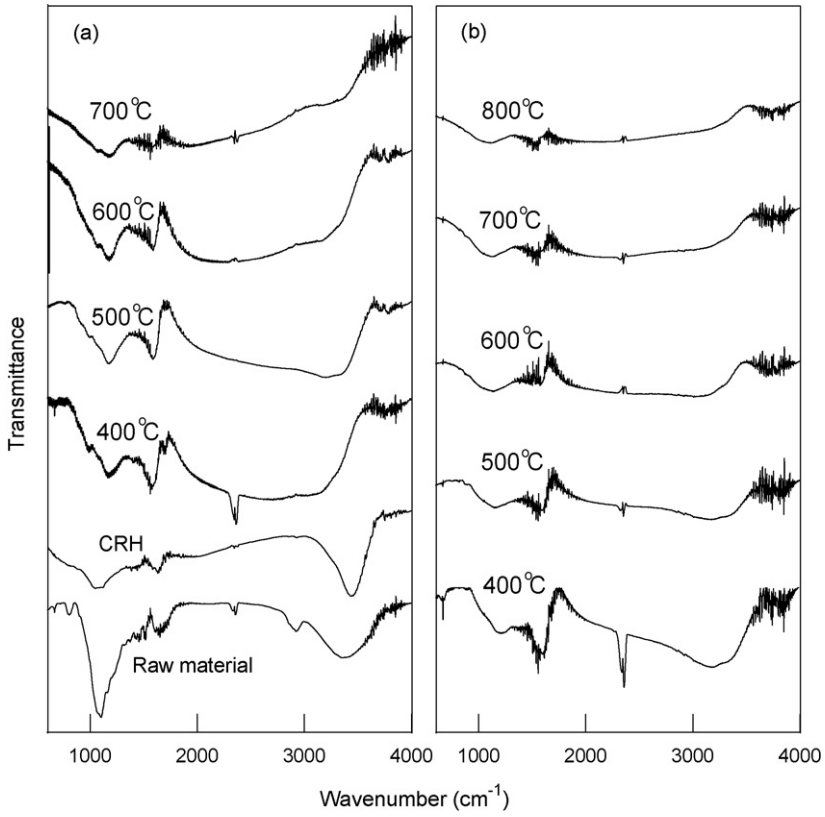

Fig. 7. FTIR spectrogram of samples: (a) H_3PO_4 activation and (b) $ZnCl_2$ activation.

the pistachio-nut shell [7], which is another type of lignocellulosic material. A wide band located about 3400 cm^{-1} is attributed to O–H hydroxyl groups or adsorbed water [35]. The band at approximately 2900 cm^{-1} corresponds to the C–H vibrations. The band at 1692 cm^{-1} is attributed to the carbonyl C=O groups. The band at about 1615 cm^{-1} may be assigned to aromatic stretching vibration of C=C. A very small peak near 1492 cm^{-1} could be attributed to $-CH_2=$ vibrations. The band at 1158 cm^{-1} may be assigned to C–O vibrations in phenols, ethers, or esters. The peak shouldered at 1051 cm^{-1} could be attributed to the alcohol R–OH groups. The bands at approximately 464, 735 and 1105 cm^{-1} are probably due to the silicon atom attached initially to the oxygen in the rice husk [11].

After carbonizing the rice husk in a N_2 atmosphere, the spectrum of CRH sample is different from the raw material. Many bands disappear, indicating the vaporization of organic matter. When rice husks are activated with H_3PO_4 and $ZnCl_2$, the bands at 464, 735, and 1105 cm^{-1} disappear completely, indicating the removal of ash in carbons. Fig. 7(a) shows that bands appear at 1692, 1564, and 1158 cm^{-1} for the H_3PO_4 activation samples, which could be attributed to C=O, C=C, and C—O vibrations, respectively. The shoulder at about 1000 cm^{-1} may be a chain of P–O–P vibration for phosphorus compounds [40]. Fig. 7(b) shows the $ZnCl_2$ activated samples, in which the bands at 1590, 1158 and a very small shoulder at 840 cm^{-1} can easily be attributed to C=C, C—O, and C—H vibrations, respectively. For both activation procedures, the intensity of these bands decreases as the activation temperature increases, indicating that the proportion of carbon content increases at high temperatures. Fig. 7 also shows that $ZnCl_2$ activated samples exhibit weaker bond intensity than H_3PO_4 activated samples. This can be explained based on the fact that the $ZnCl_2$ activation procedure has a higher proportion of carbon content than the H_3PO_4 activation procedure, which is consistent with the results of elemental analysis shown in Table 1.

Fig. 8(a) shows the morphological features of un-reacted and activated husk samples. Fig. 8 shows the outer epidermis of rice husk, which is well organized in structure that resembles rolling hills. Fig. 8(b) shows the inner surface of rice husk, which is corrugated and contains a number of rectangular tissues attached to the surface of the inner epidermis. Fig. 8(c) shows the outer epidermis of base-leached husk. The surface of the outer epidermis is peeled off, and a few big holes are present. Fig. 8(d) shows the inner epidermis of base-leached husk. The tissue of the inner epidermis looks appears clear-cut, but there are some folds on the surface. This phenomenon may be due to the fact that silica deposited in the husk is most highly concentrated in the outer epidermal tissue [41]. After base-leaching of the rice husk, the silica reacts with sodium hydroxide and is then removed by reaction (1). As a result, some large holes remain on the husk's outer epidermis. In addition, the sodium hydroxide can also decompose the lignin in the husk, causing swelling in the organic composition [42]. It is favorable to the activating agent to enter the interior of carbon tissue, as this increases the specific surface area and pore volume.

Upon activating the rice husk in N_2, Fig. 8(e) shows a morphology similar to that of the raw husk. The carbon sample appears very well organized and contains a number of nodes inlaid in the interior of tubular tissue. Fig. 8(f) shows that the appearance of ground carbon has an irregular grain. Fig. 8(g) shows that the surface of carbon activated with H_3PO_4 is covered with flakes. When rice husk is activated with $ZnCl_2$, the morphology differs from the H_3PO_4 activation sample. Fig. 8(h) shows that the strength of the carbon structure looks like hard, with a few small pores distributed within the carbon.

3.5. Thermogravimetric analysis

Fig. 9 shows the TG curves of the remaining weight (W/W_o) and DTG curves of the derivative of weight (dW/dt) for rice husk

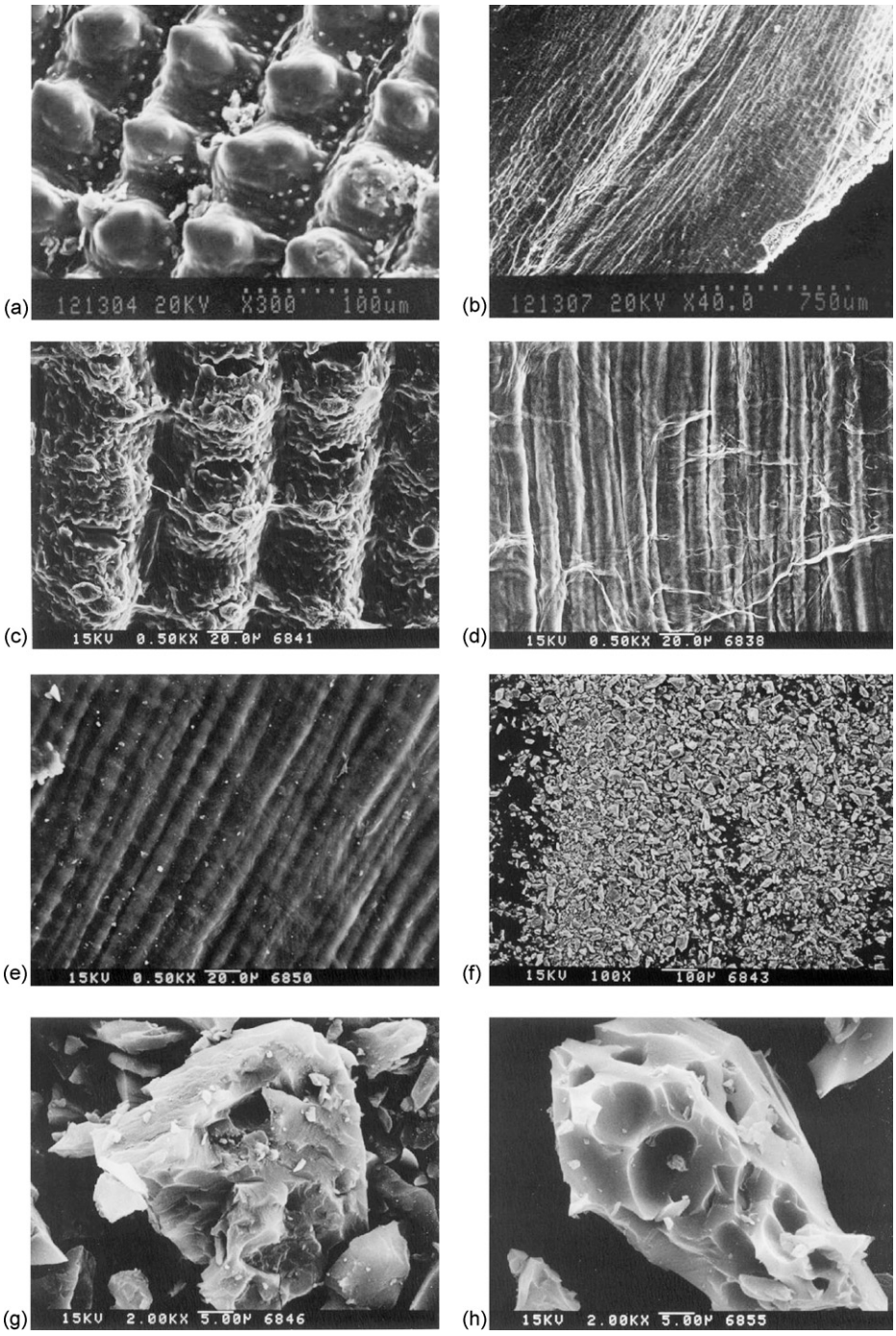

Fig. 8. Scanning electron micrographs of samples: (a) outer epidermis of rice husk, (b) inner epidermis of rice husk, (c) outer epidermis of base-leached rice husk, (d) inner epidermis of base-leached rice husk, (e) inner epidermis of activated carbon, (f) ground sample after activation reaction, (g) carbon powder by H_3PO_4 activation, and (h) carbon powder by $ZnCl_2$ activation.

activated at various impregnation ratios. Fig. 9(a) shows the TGA curve of rice husk carbonized in N_2 without any chemical activation. The mass loss occurring in the range from 100 to 375 °C may be attributed to the decomposition of organic materials. The mass loss from 375 to 800 °C corresponds to the carbonization process, which may be attributed to further pyrolysis of the intermediate [11]. Fig. 9(b) shows the TGA curves of H_3PO_4 activation. These results indicate that the mass loss of rice husk activated with H_3PO_4 occurs in three distinct temperature zones. The curves show an initial mass loss for temperature up to ~300 °C due to the volatilization of organic materials in the sample. It may be that light gases are released at relatively low temperature. A small amount of mass loss occurs in the 300–550 °C transition period, which may be associated with further thermal decomposition of organic materials rather than gasification. The temperature range of 550–900 °C corresponds to the activation process, in which mass loss may be attributed to the reaction between the activating agent and carbonaceous residue. Fig. 9(b) shows two peaks in the DTG curves. According the peak temperature at which instantaneous rate of thermal decomposition is at a maximum, the temperatures

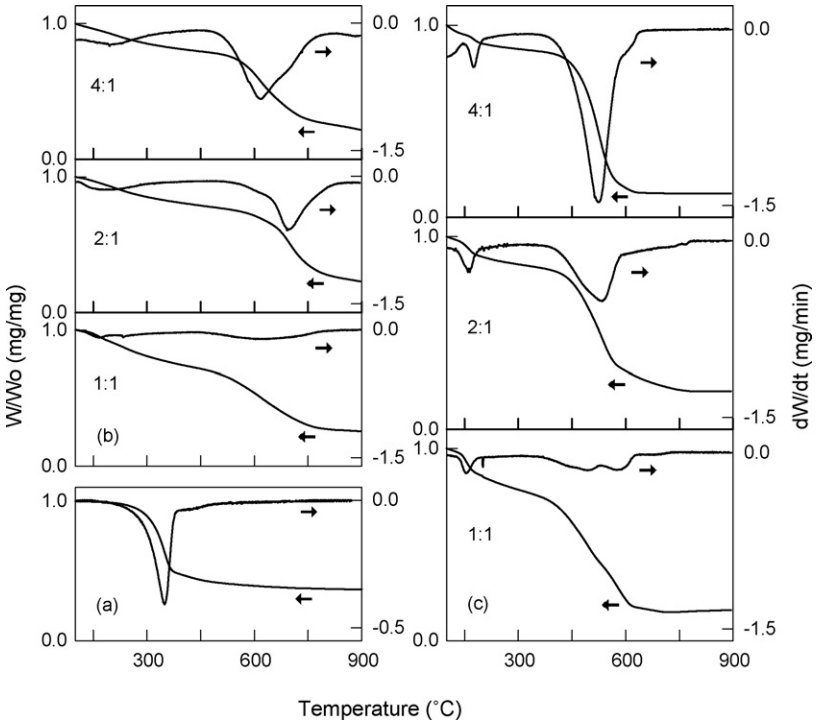

Fig. 9. TG and DTG thermograms of samples at various impregnation ratios: (a) rice husk carbonized in N_2, (b) H_3PO_4 activation and (c) $ZnCl_2$ activation.

of the first peak vary from 157 to 191 °C for the three impregnation ratios, and increase as the impregnation ratio increases. It is probable that the sample dehydration is slow when the rice husk contains a high proportion of activating agent. The temperatures of the second peak vary from 614 to 696 °C for various impregnation ratios, and increase as the impregnation ratio decreases. Simultaneously, peak high exhibits an inverse trend, and increases as the impregnation ratio increases. This indicates that the reaction rate can be increased by increasing the chemical activating agent. Hared et al. [43] reported that wood impregnated with H_3PO_4 had two peak temperatures at approximately 150–200 and 700 °C, which is consistent with the present observation.

Fig. 9(c) shows the TGA plots of $ZnCl_2$ activated rice husk obtained from various activating agent impregnation ratios. The mass loss of samples occurs in the three temperature zones, namely ~200, 200–450 and 450–800 °C. The DTG curves reveal two peak temperatures at 150–175 and 518–589 °C for the rice husk activated with $ZnCl_2$ at various impregnation ratios. The first peak temperatures increase as the impregnation ratio increases. The second peak temperatures increase as the impregnation ratio decreases. These results are similar to those of the H_3PO_4 activation procedure. Fig. 9 also shows a discrepancy between the H_3PO_4 and $ZnCl_2$ activation samples. Specifically, $ZnCl_2$ activation produces a higher mass loss and instantaneous rate of thermal decomposition. At the same time, $ZnCl_2$ activation has a lower peak temperature and shorter duration for rice-husk pyrolysis. These observations suggest that the $ZnCl_2$ activation reaction occurs faster and more easily than the H_3PO_4 activation reaction.

The activation process includes both rice husk and activating agent components. This reaction is complicated and not well understood. As mentioned earlier, the main constituents of rice husk are cellulose, hemi-cellulose and lignin. Thermogravimetric analysis shows that the activation process can be divided into three stages. This indicates that organic matter decomposes into the intermediate of smaller molar mass in the initial stage of the activation reaction. The reaction releases gaseous volatiles. Thus, the reaction mechanism at the first stage can be expressed as:

$$\text{Rice husk} \rightarrow \text{intermediate} + \text{volatiles} \quad (3)$$

During the second stage, the intermediate further decomposes to form other volatile species, tar and char. At the same time, the chemical activating agents including both $ZnCl_2$ and H_3PO_4 begin

Table 4
Reported specific surface area and pore volume of activated carbon prepared form rice husk by H_3PO_4 and $ZnCl_2$ activation.

Activating agent	Activation temperature (°C)	Impregnation ratio	BET surface area (m^2/g)	Pore volume (cm^3/g)	Researchers [Ref.]
H_3PO_4	800	4.2	379	0.373	Kennedy et al. [40]
H_3PO_4	500	–	376	0.431	Daifullah et al. [13]
H_3PO_4	400	–	649	–	Yeganeh et al. [14]
H_3PO_4	450	1.5	1295	0.735	Guo and Rockstraw [35]
H_3PO_4	500	2.0	1741	1.315	This work
$ZnCl_2$	500–550	1.0	1136	–	Usmani et al. [15]
$ZnCl_2$	600	0.1	480	1.365	Yalcin and Sevinc [16]
$ZnCl_2$	300	1.0	578	0.463	Mohanty et al. [10]
$ZnCl_2$	500	1.0	750	0.380	Kalderis et al. [17]
$ZnCl_2$	500	2.0	2434	1.344	This work

to melt or decompose [44,45]. Thus the reaction mechanisms of the second stage can be expressed as

$$\text{Intermediate} \rightarrow \text{tar} + \text{char} + \text{volatiles} \quad (4)$$

$$H_3PO_{4(s)} \rightarrow (1/2)P_2O_{5(l)} + (3/2)H_2O_{(g)} \quad (5)$$

$$ZnCl_{2(s)} \rightarrow ZnCl_{2(l)} \quad (6)$$

Note that P_2O_5 or $ZnCl_2$ acts as an oxidizing agent, and carbon acts as a reducing agent. In the third stage, the char reacts with the chemical activating agent, causing the pores to open. Finally, the solid residue regarded as activated carbon can be obtained after the washing.

Table 4 lists the specific surface area and pore volume of activated carbon obtained by the other investigators. These samples were prepared from rice husk by H_3PO_4 or $ZnCl_2$ activation. The surface area and pore volume for H_3PO_4 activation samples range from 376 to 1295 m^2/g and 0.373 to 0.735 cm^3/g, respectively. For $ZnCl_2$ activation, these values range from 480 to 1136 m^2/g and 0.380 to 1.365 cm^3/g, respectively. These values are smaller than those obtained in the current study. We therefore conclude that treating rice husk with base-leaching and acid-washing procedures promotes the activation reaction, providing high quality activated carbon powder.

4. Conclusions

This study reports the preparation of activated carbon with a high surface area and large adsorption capacity from rice husk, using H_3PO_4 and $ZnCl_2$ as the chemical activating agents. $ZnCl_2$ activation produces a higher surface area and iodine adsorption capacity than H_3PO_4 activation. The base-leaching procedure can effectively remove ash and improve the surface area and pore volume of the sample. The acid-washing procedure can act as a cleaning process to remove metallic impurities and residual activating agent. The optimum surface area of carbon for both H_3PO_4 and $ZnCl_2$ activation occurs at a temperature of 500 °C with an impregnation ratio of 2. All the samples activated at various temperatures have a turbostratic structure. Thermal analysis results show that the organic matter in the activation procedure decomposes into smaller molecules before the activation reaction. The reaction process is quite complicated, and the activation mechanism can be illustrated experimentally. The high surface area of carbon obtained from rice husk is comparable to that of other lignin–cellulose matter. Rice husk is an excellent material for the preparing activated carbon.

Acknowledgments

The authors express thanks to the National Science Council of Taiwan for its financial support under Project No. NSC 93-2214–E164–001.

References

[1] R. Baccar, J. Bouzid, M. Feki, A. Montiel, Preparation of activated carbon from Tunisian olive-waste cakes and its application for adsorption of heavy metal ions, J. Hazard. Mater. 162 (2009) 1522–1529.
[2] P.D. Tien, H. Morisaka, T. Satoh, M. Miura, M. Nomura, H. Matsui, C. Yamaguchi, Efficient evolution of hydrogen from tetrahydronaphthalene upon palladium catalyst supported on activated carbon fiber, Energy Fuels 17 (2003) 658–660.
[3] A. Anson, E. Lafuente, E. Urriolabeitia, R. Navarro, A.M. Benito, W.K. Maser, M.T. Martinez, Hydrogen capacity of palladium-loaded carbon materials, J. Phys. Chem. B 110 (2006) 6643–6648.
[4] D. Lozano-Castello, D. Cazorla-Amoros, A. Linares-Solano, Powdered activated carbons and activated carbon fibers for methane storage: a comparative study, Energy Fuels 16 (2002) 1321–1328.
[5] V. Minkova, S.P. Marinov, R. Zanzi, E. Bjornborn, T. Budinova, M. Stefanova, L. Lakov, Thermochemical treatment of biomass in a flow steam or in a mixture of steam and carbon dioxide, Fuel Process. Technol. 62 (2000) 45–52.
[6] B. Corcho-Corral, M. Olivares-Marin, C. Fernandez-Gonzalez, V. Gomez-Serrano, A. Macias-Garcia, Preparation and textural characterization of activated carbon from vine shoots (*Vitis Vinifera*) by H_3PO_4-chemical activation, Appl. Surf. Sci. 252 (2006) 5961–5966.
[7] A.C. Lua, T. Yang, Characteristics of activated carbon prepared from pistachio-nut shell by zinc chloride activation under nitrogen and vacuum conditions, J. Colloid Interface Sci. 290 (2005) 505–513.
[8] Y. Guo, S. Yang, K. Yu, J. Zhao, Z. Wang, H. Xu, Preparation and mechanism studies of rice husk based porous carbon, Mater. Chem. Phys. 74 (2002) 320–323.
[9] J.C.C. Freitas, M.A. Schettino Jr., A.G. Gunha, F.G. Emmerich, A.C. Bloise, E.R. de Azevedo, T.J. Bonagamba, NMR investigation on the occurrence of Na species in porous carbons prepared by NaOH activation, Carbon 45 (2007) 1097–1104.
[10] K. Mohanty, J.T. Naidu, B.C. Meikap, M.N. Biswas, Removal of crystal violet from wastewater by activated carbons prepared from rice husk, Ind. Eng. Chem. Res. 45 (2006) 5165–5171.
[11] T.H. Liou, Evolution chemistry and morphology during the carbonization and combustion of rice husk, Carbon 42 (2004) 785–794.
[12] T.G. Chuah, A. Jumasiah, I. Azni, S. Katayon, S.Y. Thomas Choong, Rice husk as a potentially low-cost biosorbent for heavy metal and dye removal: an overview, Desalination 175 (2005) 305–316.
[13] A.A.M. Daifullah, B.S. Girgis, H.M.H. Gad, A study of the factors affecting the removal of humic acid by activated carbon prepared from biomass materials, Colloid Surf. A-Physicochem. Eng. Asp. 235 (2004) 1–10.
[14] M.M. Yeganeh, T. Kaghazchi, M. Sileimani, Effect of raw materials on properties of activated carbons, Chem. Eng. Technol. 29 (2006) 1247–1251.
[15] T.H. Usmani, T.W. Ahmad, A.H.K. Yousufzai, Preparation and liquid-phase characterization of granular activated-carbon from rice husk, Bioresour. Technol. 48 (1994) 31–35.
[16] N. Yaclin, V. Sevinc, Studies of the surface area and porosity of activated carbons prepared from rice husks, Carbon 38 (2000) 1943–1945.
[17] D. Kalderis, S. Bethanis, P. Paraskeva, E. Diamadopoulos, Production of activated carbon from bagasse and rice husk by a single-stage chemical activation method at low retention times, Bioresour. Technol. 99 (2008) 6809–6816.
[18] J.B. Castro, P.R. Bonelli, E.G. Cerrella, A.L. Cukierman, Phosphoric acid activation of agricultural residues and bagasse from sugar cane: influence of the experimental conditions on adsorption characteristics of activated carbons, Ind. Eng. Chem. Res. 39 (2000) 4166–4172.
[19] D.C.C. Azevedo, J.C.S. Araujo, M. Bastos-Neto, A.E.B. Torres, E.F. Jaguaribe, C.L. Cavalcante, Microporous activated carbon prepared from coconut shells using chemical activation with zinc chloride, Micropor. Mesopor. Mater. 100 (2007) 361–364.
[20] C.H. Yun, Y.H. Park, G.H. Oh, C.R. Park, Contribution of inorganic components in precursors to porosity evolution in biomass-based porous carbons, Carbon 41 (2003) 2009–2025.
[21] D. Lozano-Castello, M.A. Lillo-Rodenas, D. Cazorla-Amoros, A. Linares-Solano, Preparation of activated carbons from Spanish anthracite I. activation by KOH, Carbon 39 (2001) 741–749.
[22] X. Zhang, L. Lei, Effect of preparation methods on the structure and catalytic performance of TiO_2/AC, J. Hazard. Mater. 153 (2008) 827–833.
[23] E. Carpio, P. Zuniga, S. Ponce, J. Solis, J. Rodriguez, W. Estrada, Photocatalytic degradation of phenol using TiO_2 nanocrystals supported on activated carbon, J. Mol. Catal. A-Chem. 228 (2005) 293–298.
[24] H. Fan, Q. Xu, Y. Guo, O. Peng, Z. Hou, Nanoporous ferric oxide prepared with activated carbon template in supercritical carbon dioxide, Mater. Sci. Eng. A-Struct. Mater. Prop. Microstruct. Process. 422 (2006) 272–277.
[25] S.J. Park, Y.S. Jang, Preparation and characterization of activated carbon fibers supported with silver metal for antibacterial behavior, J. Colloid Interface Sci. 26 (2003) 238–243.
[26] T.H. Liou, F.W. Chang, J.J. Lo, Pyrolysis kinetics of acid-leached rice husk, Ind. Eng. Chem. Res. 36 (1997) 568–573.
[27] S. Brunauer, P.H. Emmett, E. Teller, Adsorption of gases in multimolecular layers, J. Am. Chem. Soc. 60 (1938) 309–319.
[28] M.M. Dubinin, Fundamentals of the theory of adsorption in micropores of carbon adsorbents: characteristics of their adsorption properties and microporous structures, Carbon 27 (1989) 457–467.
[29] C.H. Yun, Y.H. Park, C.R. Park, Effects of pre-carbonization on porosity development of activated carbons from rice straw, Carbon 39 (2001) 559–567.
[30] T.H. Loiu, Pyrolysis kinetics of electronic packaging material in a nitrogen atmosphere, J. Hazard. Mater. B 103 (2003) 107–123.
[31] M.A. Hamad, Thermal characteristics of rice hulls, J. Chem. Technol. Biotechnol. 31 (1981) 624–626.
[32] Q. Tang, T. Wang, Preparation of silica aerogel from rice hull ash by supercritical carbon dioxide drying, J. Supercrit. Fluids 35 (2005) 91–94.
[33] S. Timur, I.C. Kantarli, E. Ikizoglu, J. Yanik, Preparation of activated carbons from Oreganum stalks by chemical activation, Energy Fuels 20 (2006) 2636–2641.
[34] G.H. Oh, C.R. Park, Preparation and characteristics of rice-straw-based porous carbons with high adsorption capacity, Fuel 81 (2002) 327–336.
[35] Y. Guo, D.A. Rockstraw, Activated carbons prepared from rice hull by one-step phosphoric acid activation, Micropor. Mesopor. Mater. 100 (2007) 12–19.
[36] L.J. Kennedy, K. Mohan das, G. Sekaran, Integrated biological and catalytic oxidation of organics/inorganics in tannery wastewater by rice husk based mesoporous activated carbon-*Bacillus* sp., Carbon 42 (2004) 2399–2407.
[37] S.J. Gregg, K.S.W. Sing, Adsorption, Surface Area and Porosity, Second ed., Academic Press, London, 1982.

[38] Z. Hu, M.P. Srinivasan, Mesoporous high-surface-area activated carbon, Micropor. Mesopor. Mater. 43 (2001) 267–275.
[39] N. Iwashits, C.R. Park, H. Fujimoto, M. Shiraishi, M. Inagaki, Specification for a standard procedure of X-ray diffraction measurements on carbon materials, Carbon 42 (2004) 701–714.
[40] L.J. Kennedy, J.J. Vijaya, G. Sekaran, Effect of two-stage process on the preparation and characterization of porous carbon composite from rice husk by phosphoric acid activation, Ind. Eng. Chem. Res. 43 (2004) 1832–1838.
[41] N.K. Sharma, W.S. Williams, A. Zangvil, Formation and structure of silicon carbide whiskers from rice hulls, J. Am. Ceram. Soc. 67 (1984) 715–720.
[42] M. Rao, A.V. Parwate, A.G. Bhole, Removal of Cr^{6+} and Ni^{2+} from aqueous solution using bagasse and fly ash, Waste Manage. 22 (2002) 821–830.
[43] I.A. Hared, J.L. Dirion, S. Salvador, M. Lacroix, S. Rio, Pyrolysis of wood impregnated with phosphoric acid for the production of activated carbon: kinetics and porosity development studies, J. Anal. Appl. Pyrolysis 79 (2007) 101–105.
[44] M. Olivares-Marin, C. Fernandez-Gonzalez, A. Macias-Garcia, V. Gomez-Serrano, Thermal behavior of lignocellulosic material in the presence of phosphoric acid. Influence of the acid content in the initial solution, Carbon 44 (2006) 2330–2356.
[45] Q. Qian, M. Mochida, H. Tatsumoto, Preparation of activated carbons from cattle-manure compost by zinc chloride activation, Bioresour. Technol. 98 (2007) 353–360.